

Sterically stabilized superparamagnetic liposomes for MR imaging and cancer therapy: Pharmacokinetics and biodistribution

V. Plassat ^a, M.S. Martina ^a, G. Barratt ^a, C. Ménager ^b, S. Lesieur ^{a,*}

^a Laboratoire Physico-Chimie Pharmacotechnie Biopharmacie, UMR CNRS 8612, Faculté de Pharmacie, Université Paris-Sud, 5 rue Jean-Baptiste Clément, F-92296 Châtenay-Malabry Cedex, France

^b Laboratoire des Liquides Ioniques et Interfaces Chargés, UMR CNRS 7612, Université Pierre et Marie Curie, case 63, 4 place Jussieu, F-75252 Paris Cedex, France

Received 16 February 2007; received in revised form 27 April 2007; accepted 1 May 2007

Available online 17 May 2007

Abstract

Pharmacokinetics of magnetic-fluid-loaded liposomes (MFLs) with mean hydrodynamic diameter of 200 nm sterically stabilized by poly(ethylene glycol) (PEG) and labelled by a fluorescent lipid probe, *N*-(lissamine rhodamine B sulfonyl) phosphatidylethanolamine (Rho-PE) was studied. The loading consisted in an aqueous suspension of maghemite nanocrystals close to 8 nm in size at 1.7 Fe(III) mol/mol total lipids ratio. Double tracking of MFL in blood was performed versus time after intravenous administration in mice. Lipids constituting vesicle membrane were followed by Rho-PE fluorescence spectroscopy while iron oxide was determined independently by relaxometry. MFLs circulating in the vascular compartment conserved their vesicle structure and content. The pharmacokinetic profile was characterized by two first-order kinetics of elimination with distinct plasmatic half-lives of 70 min and 12.5 h. Iron biodistribution and organ histology clearly highlighted preferential MFL accumulation within liver and spleen. The pathway in spleen supported that elimination was governed by the mononuclear phagocyte system (MPS). PEG coating was essential to prolong MFL circulation time whereas iron oxide loading tends to favour uptake by the MPS. Despite partial uptake in the earlier times after administration, MFLs exhibited long circulation behaviour over a 24-h period that, coupled to magnetic targeting, encourages further use in drug delivery.

© 2007 Elsevier B.V. All rights reserved.

Keywords: Magnetic-fluid loaded liposomes; Fluorescence; Relaxometry; Ferrofluid; Histology; Long-circulating vesicles

1. Introduction

Severe side toxic effects and rather long treatment durations are vexing drawbacks in the use of conventional chemotherapeutics. Carrier systems for selective delivery of anticancer drugs have been widely developed to reduce the doses administered to the patients by improving drug stability and circulation times while promoting preferential distribution in the site of organism to be treated. Lipid vesicles or liposomes are especially competitive to date as the most clinically established nanometer-scale particles for the delivery of cytotoxic chemicals, genes, vaccines or agents for medical imaging (Lasic, 1998; Torchilin, 2005; Allen and Cullis, 2004). The biomedical interest of these colloids mainly relies on their biocompatible properties but also

on their encapsulating behaviour of indifferently hydrophilic or lipophilic substances and possibility of being surface-modified. For nearly four decades, a number of works have notably been focusing on liposomes sterically stabilized by grafting hydrophilic poly(ethylene glycol) (PEG) chains onto their lipid bilayer. PEGylated liposomes of small size (100–200 nm in diameter), also called Stealth® liposomes, exhibit longer circulating times and reduced uptake by the mononuclear phagocyte system (MPS) constituting a major breakthrough in therapeutics as they can be distributed to tissues other than the MPS. Long-circulating liposomes have shown extravasation in tissues with enhanced vascular permeability and increased accumulation in solid tumors (Papahadjopoulos et al., 1991), but at rates often not sufficient for therapeutic efficacy of the delivered drug.

To optimize liposome-carried drug concentrations in diseased tissues, active targeting has been envisaged by coupling to the surface-coating PEG chains ligands like antibodies, peptides or any other small molecules capable of increasing

* Corresponding author. Tel.: +33 1 46 83 53 49; fax: +33 1 46 83 53 12.
E-mail address: sylviane.lesieur@u-psud.fr (S. Lesieur).

liposome-cell association (Leserman et al., 1980). Another possible strategy is physical targeting of drugs by magnetic guidance (Shinkai and Ito, 2004; Nobuto et al., 2004; Kuznetsov et al., 2001). Therefore, for several years, we have been developing unilamellar phospholipid vesicles with a mean diameter of about 200 nm, loaded with superparamagnetic nanocrystals of maghemite. These magnetic-fluid-loaded liposomes (MFL) have been specifically designed to enable both magnetic resonance imaging (MRI) and magnetic targeting *in vivo* after systemic administration. The lipid composition has been optimized by surface-grafted poly(ethylene glycol) (PEG) chains to obtain sterically stabilized liposomes which avoid rapid uptake by the MPS (Lesieur et al., 2003; Martina et al., 2005). A rhodamine-labelled phospholipid *N*-(lissamine rhodamine B sulfonyl) phosphatidylethanolamine (Rho-PE) was included in the bilayer to allow *in vitro* and *in vivo* fluorescence microscopy imaging (Martina et al., 2007). Our results have clearly ranked them among the best T_2 MRI contrast agents existing to date, with the advantages of being non-toxic, long-circulating in blood and displaying magnetophoretic mobility. The latter has been successfully exploited to target different tissues *in vivo*, especially solid tumors and brain, by applying an external magnetic field gradient to the region of interest (Fortin et al., 2006; Riviere et al., *in press*). These encouraging results prompted us to use MFLs not only as magnetically guided diagnosis agents but also as tool for targeting of drugs that could be co-encapsulated with the magnetic fluid and then carried within the vesicle structure under the influence of an external magnetic field. For this application, it is important to know the bioavailability and tissue distribution of MFLs after intravenous administration. In particular, the effect of loading liposomes with high maghemite concentrations on their clearance has been never studied before.

This work presents the pharmacokinetics and *in vivo* tissue distribution of PEG-ylated MFLs after intravenous injection in mice, in the absence of magnetic targeting. Fluorescent labeling of the lipid bilayer by Rho-PE and the magnetic properties of the entrapped iron oxide allowed the bilayer shell and the internal content of the liposomes to be followed simultaneously, indicating whether the structural integrity of the circulating MFLs was conserved in blood stream or not. Lipids constituting the vesicle bilayer were measured by fluorescence spectroscopy while the magnetic fluid was followed by measuring the spin-spin relaxation time of water protons. The distribution of MFLs within different organs was examined by determining the amounts of iron oxide accumulated in the tissues and by visualization of the rhodamine-labeled vesicle pathway as a function of time by confocal fluorescence microscopy.

2. Materials and methods

2.1. Materials

Chloroform solutions of egg-yolk-extracted L- α -phosphatidylcholine (EPC), 1,2-diacyl-SN-glycero-3-phosphoethanolamine-*N*-(methoxy(poly(ethylene glycol))-2000) (DSPE-PEG₂₀₀₀) and *N*-(lissamine rhodamine B sulfonyl) phosphatidylethanolamine (Rho-PE) were purchased from Avanti

Polar Lipids (Alabaster, AL). Sodium chloride, sodium citrate and *N*-(2-hydroxyethyl)piperazine-*N'*-[2-ethanesulfonic acid] (HEPES), octyl- β -D-glucopyranoside (octyl glucoside, OG) were provided by Sigma (St. Louis, MO). Unless otherwise stated, the buffer used was 108 mM NaCl, 20 mM sodium citrate, 10 mM HEPES, pH 7.4 and 285 mOsm (measured with a cryoscopic micro-osmometer, Bioblock Scientific, France).

2.2. Magnetic-fluid-loaded liposome preparation

Nanocrystals of maghemite (γ -Fe₂O₃) were synthesized according to Massart's method (Massart, 1982). Final adjustment of both aqueous medium and maghemite concentration (5.0 M Fe(III) by flame spectroscopy) was performed by ultrafiltration through a MACROSEP filter, cut-off 50 kD (Fisher Scientific Labosi, France) as previously described (Martina et al., 2005).

Rhodamine-labeled magnetic-fluid-loaded liposomes (MFLs) were prepared by hydration of a thin lipid film (EPC:DSPE-PEG₂₀₀₀:Rho-PE; 94:5:1 mol% or EPC:Rho-PE; 99:1 mol% for PEG-ylated or conventional MFLs) by adding equal volumes of the suspension of maghemite particles and buffer to get a total lipid concentration of 20.0 ± 0.8 mM (checked by enzymatic assay, Phospholipides Enzymatiques PAP 150, Biomérieux, France) followed by sequential extrusion (nitrogen pressure <10 bars, 25 °C) through polycarbonate filters with decreasing pore diameters of 0.8 μ m/0.4 μ m/0.2 μ m (PORETICS, Osmotics, Livermore, USA). Non-entrapped maghemite particles were removed by gel exclusion chromatography (GEC) performed with a 0.4 cm \times 5.8 cm Sephadryl S1000 superfine (Pharmacia) microcolumn (TERUMO 1 mL-syringe) beforehand saturated with EPC: DSPE-PEG₂₀₀₀ (95:5 mol%) liposomes, prepared similarly to MFLs but without maghemite. The eluent was the buffer used for liposome preparation. MFLs with lower maghemite loadings were obtained by the same procedure except that the lipid film was hydrated by replacing part of the magnetic fluid by buffer to get the desired final iron oxide content while maintaining total lipid concentration at 20 mM. Final Fe(III) concentrations in the sample preparations (from 20.0 to 68.0 ± 1.3 mM) were checked by flame spectroscopy. Liposomes with loading of 1.0, 1.7 and 3.4 moles of iron oxide per mole of lipid were prepared.

The hydrodynamic diameters of the final MFLs were determined by quasi-elastic light scattering (QELS) with a Nanosizer apparatus (N4 MD, Coultronics), at 25 °C, 90° scattering angle and using size distribution processor (SDP) analysis (total lipid concentration: 0.15 mM). Fluorescence spectroscopy and confocal microscopy were performed using the procedures described below in Sections 2.4 and 2.5. Zeta potential measurements were performed at 25 °C by using a zetasizer apparatus (Malvern Instruments SA, France).

2.3. Animal experiments

Animal experiments were carried out in accordance with the recommendations of the EEC (86/609/CEE) and the French National Committee (decree 86/848) for the care and use of

laboratory animals. Six-week-old female CD 1 mice weighing 27.6 ± 1.7 g (2.1 mL blood volume from Sluiter et al., 1984) were used in the pharmacokinetic experiments (Charles River Laboratories, Les Oncins, France). Mice were separated into groups of three (not injected, 2-h and 8-h groups) or six (other time points) animals and housed in metabolism cages. Food and water were given *ad libitum*. The animal room was kept at a controlled temperature (22 °C) and light cycle (12 h light exposure from). Before injecting the mice into the retro-orbital sinus (200 µL MFL, 20 mM total lipids, 34 mM Fe(III), 14 µg iron per g of mouse), they were anesthetized by placing them for 5 min in an induction chamber filled with 3.5% (v/v) in air of isoflurane AErrane® (Pharmacia, France) at a rate of 1 L per minute. During injection (around 10 s), anesthesia was maintained by inhalation of 2.5% (v/v) isoflurane/air (0.5 L/min) by using a respirator. The mice were returned to their room between recovering from anesthesia and blood and organ sampling.

Five minutes before each time-point, the animals were anesthetized as described above. Then, 100 and 200 µL of total blood samples were taken by cardiac puncture for separate analysis of lipids and iron oxide and immediately mixed with 1 mL and 500 µL, respectively, of 60 mM sodium citrate solution, to prevent coagulation. Citrate-treated blood samples were stored at 4 °C until analyses which were performed within the next 6 h for lipids and within less than 48 h for iron oxide.

After blood sampling, the mice were sacrificed by cervical rupture under anesthesia and organs (liver, spleen, heart, kidneys, lungs) were carefully removed and placed in 4% paraformaldehyde (v/v in 1X phosphate buffer saline PBS Gibco®) at 4 °C, pH 7.4, for 4 days. Then organs were rinsed with and stored in 1X PBS at 4 °C. Buffer was changed once after 24-h storage.

2.4. Magnetic fluid biodistribution and histological analyses

Separate weighed portions of the organs were taken for iron content measurement and histological analysis. Iron content was determined by atomic absorption spectrometry (AAnalyst 100, Perkin Elmer, France). Organ pieces in the range of 10–20% (20–30% for livers) by weight of total organ (10^{-5} g weight precision) were introduced into a 4 mL vial with 0.5 mL (1 mL for liver pieces) aqueous chlorhydric acid 35% (v/v) and 0.25 mL (0.5 mL for liver pieces) aqueous sulfuric acid 90% (v/v) and placed in a sonication bath (B 2200, Bransonic, France) for 2 h until complete dissolution. Then, 300 µL aliquots of the obtained homogenous mixtures were diluted in 2.5 mL distilled water and directly analyzed. The iron contents (precision, 1.68×10^{-8} mol) were determined with 9% standard deviation ($n = 3$) by using a standard linear curve in the 10 to 100 µg/mL range (0.99 correlation coefficient), independently established from known iron oxide solutions in the same solvent. Organ extracts for histology were put in 8 mL poly(ethylene) boxes filled with OCT (optimum cutting temperature, Compound Gurr®, BDH, England) and then plunged into liquid nitrogen for 2 min. Freeze tissue blocks were cut in a cryomicrotome (CM 3050S, Leica, Germany) at -21 °C into 18–20 µm thick sections. These were observed by confocal fluorescence

microscopy using a CLSM 510 microscope (Zeiss, Germany) coupled with a LSM 5 Image Browser (Zeiss, Germany) and an air-cooled ion laser providing excitation light at 488 and 543 nm. Before analysis, a drop of Slowfade® (Molecular Probes, USA) was deposited on the slices to ensure fluorescence protection. Images were obtained by using Plan Apochromat 14× and 20× objective lens (Zeiss, Germany) and 505–550 and 563–659 nm emission filters. Pictures seen in Figs. 8 and 9 were representative of a number of images from three sections per mouse organ each taken from three distinct animals.

2.5. Lipids pharmacokinetics by fluorescence spectroscopy

Fluorescence emission spectroscopy was carried out on a spectrofluorimeter (Fluorolog Spex FL1T11, Jobin Yvon, Longjumeau, France) connected to a computer. Standards were obtained by addition of known amounts of the MFL preparation used for animal injections to blood taken from the group of non-injected mice. Just before each fluorescence measurement, 600 µL of 60 mM sodium citrate and 100 µL of 100 mM OG aqueous solutions were added to the blood samples previously treated by sodium citrate (see Section 2.3). Then, 250 µL of the diluted blood sample was added into 1.750 mL of 33 mM octyl glucoside (OG) and 60 mM sodium citrate solution in water to obtain complete solubilization of both MFLs and blood components. The final optically transparent solutions (2 mL) were then placed in a 1-cm path length quartz cell maintained at 20 °C. Rho-PE fluorescence emission spectra were recorded between 585 and 700 nm at 569 nm excitation wavelength. The average emission spectrum of three liposome-free blood samples at the same blood concentration and similarly treated by sodium citrate and OG was subtracted from the sample and standard emission spectra. Lipid concentrations (0.5 nM Rho-PE detection limit) were determined from the standard linear curve giving the variation of intensity at the maximum emission wavelength (590 ± 2 nm) versus Rho-PE concentration in the 1–100 nM range (0.99 correlation coefficient). Each sample analysis was performed in triplicate (8% standard deviation).

2.6. Magnetic fluid pharmacokinetics by relaxometry

T_2 relaxation times were measured at 0.47 T (20 MHz proton Larmor frequency) and 37 °C using a Minispec PC120 spectrometer (Bruker, France), using a Carr-Purcell Meiboom Gill (CPMG) spin echo pulse sequence (interpulses delay of 1 ms, 100 data points, 5 acquisitions). Just before each measurement, 500 µL of a 60 mM sodium citrate and 66 mM OG aqueous solution was added to the blood samples previously treated by sodium citrate (see Section 2.3). Then, 200 µL of the diluted blood sample was added into 1.0 mL of 33 mM octyl glucoside (OG) and 60 mM sodium citrate solution in water to get complete solubilization of both MFLs and blood components. Standards were prepared similarly by mixing known amounts of the MFL dispersion used for animal injections with blood taken from non-injected mice. Average iron oxide contents (1.4 µM precision; 4% standard deviation, $n = 3$) were calculated from the $1/T_2$ versus $[\text{Fe(III)}]$ standard linear curve in the 2.8–285 µM

Fe(III) concentration range (0.99 correlation coefficient).

3. Results

3.1. MFL characteristics

The PEG-ylated and rhodamine-labeled magnetic-fluid-loaded liposomes (MFLs) prepared in this study were homogenous in size with a mean hydrodynamic diameter of 200 ± 40 nm from QELS, in good agreement with our earlier results (Riviere et al., in press; Martina et al., 2007). Insertion of Rho-PE into the membrane rendered the liposomes fluorescent properties to the liposomes which exhibited maximum excitation and emission intensity at 569 and 592 nm, respectively, independently of magnetic fluid encapsulation (Fig. 1). The high fluorescence yield is shown by the confocal fluorescence microscopy image in Fig. 2, which also reveals well individualized and rather monodisperse particles. For the pharmacokinetic experiments, the amount of magnetic fluid entrapped within the vesicles was fixed to that already proved to be efficient for magnetic direction *in vitro* and *in vivo*, i.e., equal to 1.7 mol of Fe(III) per mole of lipids and 2.5 M maghemite internal concentration (Martina et al., 2005, 2007; Fortin et al., 2006; Riviere et al., in press). In these conditions, MFLs are stable over more than 3 months in different aqueous media, even in the presence of serum (Martina et al., 2005).

3.2. *In vivo* pharmacokinetics

MFL were followed in the blood of mice by both the Rho-PE fluorescence in the lipid bilayer and by relaxometry for the entrapped maghemite particles. In the first case, in order to accurately quantify Rho-PE concentrations in blood by fluorescence spectroscopy, it was necessary to eliminate the inner filter effect (Lakowicz, 1983) mainly due to the presence of erythrocytes and serum proteins in the samples. This was achieved by solubilisation with the non-ionic surfactant octyl glucoside (OG) that does not interfere with fluorescent characteristics of the probe

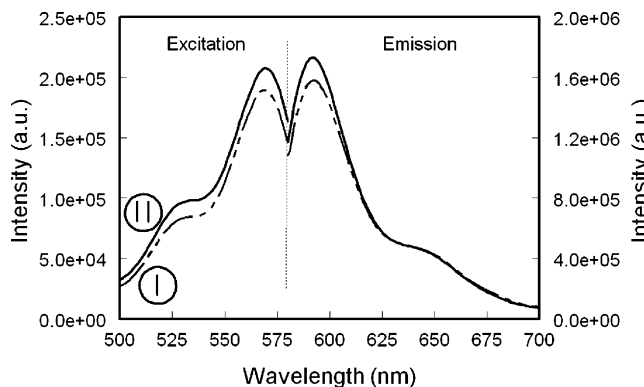


Fig. 1. Fluorescence excitation (596 nm emission wavelength) and emission (569 nm excitation wavelength) spectra in buffer at 25 °C of (EPC:DSPE-PEG₂₀₀₀:Rho-PE; 94.5:1 mol%) liposomes (0.2 mM total lipid concentration) with (I) or without (II) magnetic fluid at 2.5 M internal concentration. Liposomes mean hydrodynamic diameters from QELS were 200 ± 40 nm (I) and 190 ± 50 nm (II).

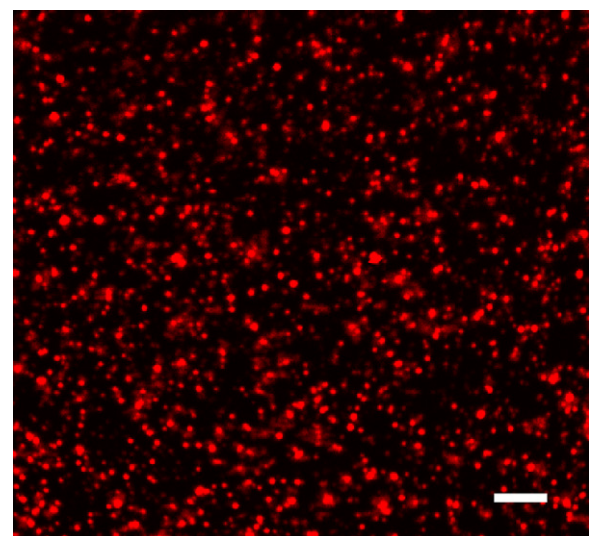


Fig. 2. Confocal microscopy image of (EPC:DSPE-PEG₂₀₀₀:Rho-PE; 94.5:1 mol%) magnetic-fluid-loaded liposomes (5×10^{-2} mM total lipid). Incident ion-laser wavelength: 543 nm. White bar: 2 μ m. Liposomes are seen with an apparent size higher than their effective diameter due to superimposed Rayleigh scattering (Martina et al., 2005, 2007).

and dissolve lipid and serum components without causing precipitation (Morandat and El Kirat, 2007). UV-visible absorption spectra before and after addition of OG to blood taken from non-injected mice clearly demonstrated effective solubilisation by this surfactant. The baseline level became very low, indicating that blood turbidity was largely eliminated. Only the absorption bands of haemoglobin at 539 and 574 nm persisted. In these conditions, the samples became optically transparent, thus allowing fluorescence measurements. Fig. 3 shows fluorescence emission spectra of Rho-PE recorded from OG-solubilized MFLs at a 2 μ M total lipid concentration, either in buffer (spectrum I) or in blood before (spectrum II) and after (spectrum III) subtracting the emission spectrum of OG-treated blood (IV) at the same dilution. It is noteworthy that the subtracted Rho-PE spectrum in blood is similar in shape to that in buffer and will be

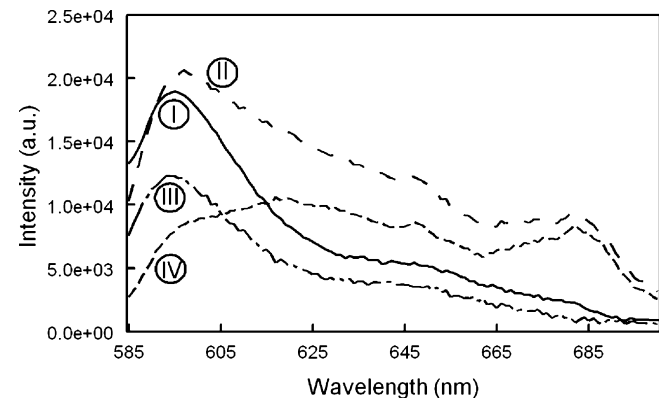


Fig. 3. Fluorescence emission spectra recorded from rhodamine-labeled magnetic-fluid-loaded liposomes in a 33 mM OG solution in buffer (I) or in blood treated by a 60 mM sodium citrate and 33 mM OG solution at 0.5% (v/v) dilution ratio (II). Total lipid concentration: 2 μ M. Spectrum (III) was obtained by subtracting the emission spectrum (IV) of blood solubilized in 60 mM sodium citrate and 33 mM OG (0.5%, v/v dilution ratio).

easily detected at submicromolar concentrations, providing efficacy of solubilisation with OG. Nevertheless, the intensities at the emission maximum of the probe differ due to residual inner filter effect of haemoglobin absorption in the rhodamine excitation and emission ranges. For this reason, samples taken from injected mice and standards were analyzed at a rigorously fixed blood dilution ratio, i.e., at a constant inner filter effect.

Samples for magnetic fluid titration by relaxometry were similarly solubilised by OG to obtain a homogenous distribution of the maghemite nanocrystals and hence a reliable response in the relaxation time shortening of the hydrogen nuclei as a function of iron oxide concentration. In such conditions, the transverse relaxation kinetics could be simply described by the following equation (Okuta, 1999):

$$\frac{1}{T_2} = \frac{1}{T_{2\text{ sol}}} + r_2 \times [\text{Fe(III)}] \quad (1)$$

where T_2 is the transverse relaxation time of the protons in the presence of magnetic fluid that acts as contrast agent, $T_{2\text{ sol}}$ the transverse relaxation time of water protons in the iron-free blood solution, and coefficient r_2 is the proton relaxation rate or relaxivity. The r_2 value found from linear regression analysis of standard measurements was equal to $29 \pm 2 \text{ mM}^{-1} \text{ s}^{-1}$ that was about three times lower than the value previously determined in buffer medium ($108 \pm 5 \text{ mM}^{-1} \text{ s}^{-1}$) (Martina et al., 2005). This was probably because the medium containing blood was more viscous than the aqueous buffer.

Fig. 4 shows the correlation between Rho-PE and Fe(III) concentrations independently determined at different times after intravenous injection of MFLs to mice. A linear relationship clearly existed and regression analysis gave a slope of the straight line equal to 1.75 (0.97 correlation coefficient) that was, within the experimental error, equal to the value of the initial encapsulation ratio of the injected MFLs (1.7 ± 0.1). It then appeared that the amount of iron oxide per unit of lipid circulating in the vascular compartment was both independent of time and,

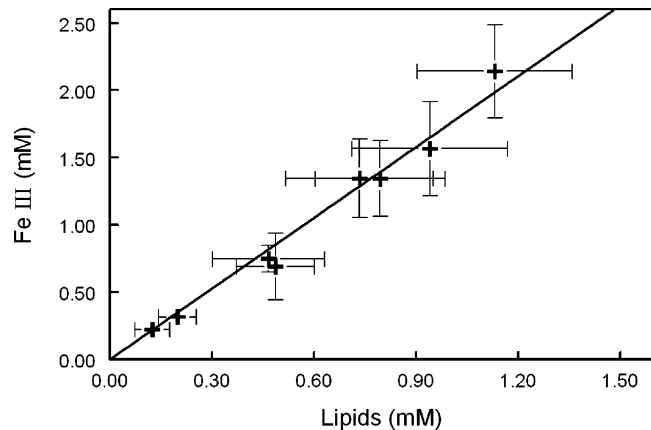


Fig. 4. Variation of iron oxide concentrations determined by relaxometry versus total lipid concentrations from Rho-PE fluorescence measurements in blood samples taken from mice at different time intervals (0.25; 0.5; 0.75; 1; 2; 4; 8; 24 h) after intravenous injection of magnetic-fluid-loaded liposomes (246 μmol iron oxide and 145 μmol lipids per kg). Points are the mean values for six animals with the exception of those at 2 and 8 h (mean for three animals).

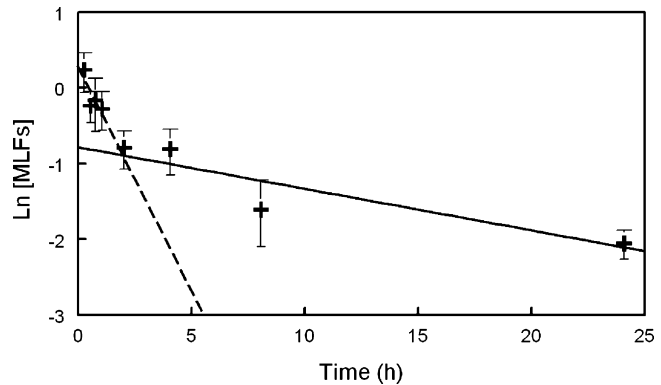


Fig. 5. Blood concentrations of magnetic-fluid-loaded liposomes, expressed in Naperian logarithm of total lipid concentration (mM) as a function of time after intravenous injection to mice (246 μmol iron oxide and 145 μmol lipids per kg). The value at each time-point corresponds to the average of the data obtained from Rho-PE fluorescence measurements and from relaxometry by dividing iron oxide levels by the slope of the straight line in Fig. 4. These are the mean values for six animals with the exception of points at 2 and 8 h (mean for three animals). The straight lines are drawn by using the parameters calculated from the best double exponential fitting of the data ($1.35 \exp(-0.59t)$ and $0.43 \exp(-0.055t)$, respectively).

importantly, the same as that initially injected. A Student's test performed over the different mice groups of mice confirmed the iron-lipid correlation with a risk below 5%.

On the basis of the preceding result, intravascular concentrations of iron oxide or Rho-PE could be used indifferently to calculate the concentrations of the circulating magnetic-fluid-loaded liposomes. Thus, these data were compiled to establish the pharmacokinetic profile shown in Fig. 5. This profile was characteristic of biphasic elimination from blood that consisted in a rapid elimination phase of MFLs within the first two hours followed by a much slower elimination phase, MFLs being still detected in blood 24 h after injection. Double exponential fitting demonstrated the existence of two first-order elimination (Log-linear) kinetics with rate constants of 9.95×10^{-3} and $9.16 \times 10^{-4} \text{ min}^{-1}$, respectively, yielding distinct intravascular half-lives of 70 min and 12.6 h.

To investigate the role of PEG coating and that of iron oxide loading on liposomes clearance from blood, PEG-ylated rhodamine-labelled liposomes with different iron loadings were prepared, as well as conventional (non PEG-ylated) liposomes with or without iron oxide. The intravascular lipid concentrations were determined by Rho-PE fluorescence spectrometry 4 h after injection. As shown in Fig. 6, a large proportion of the liposomes without PEG coating had been cleared from the blood at this time, the magnetic-fluid-loaded ones being hardly detectable. In contrast, significant amounts of the PEG-ylated liposomes remained in blood. However empty liposomes seemed to circulate longer than MFLs which, furthermore, were cleared in the same way whatever their magnetic fluid content.

3.3. Tissue distribution and histology

Tissue distribution of iron oxide entrapped in MFLs and injected intravenously into mice was studied at different times after injection. Fig. 7 shows results from atomic absorption

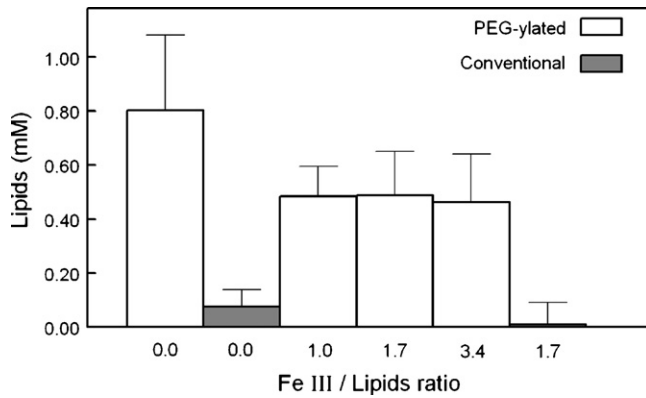


Fig. 6. Variation of liposome concentration (mM total lipids from Rho-PE fluorescence spectrometry) in blood 4 h after intravenous injection to mice (145 μ mol lipids per kg) as a function of iron oxide loading and coating. Numbers in abscissa indicate iron loading in moles of Fe(III) per mole of lipids. QELS hydrodynamic diameters of liposomes from the left to the right: 200 ± 45 , 300 ± 60 , 190 ± 40 , 190 ± 50 , 200 ± 50 , 290 ± 55 nm. Each bar is the mean value for three (PEG-ylated MFLs with 1.0 or 3.4 mol of iron per mole of lipid) or six (others) animals.

spectrometry for heart, liver, lungs, spleen and kidneys. They clearly highlighted preferential and progressive accumulation within liver and spleen in agreement with uptake of MFLs by mononuclear phagocyte system. The other organs showed iron contents that were not significantly different from that of untreated mice. The slight uptake by kidneys from 4 h onwards may be related to the physiological iron excretion pathway (Canonne-Hergaux and Gros, 2002).

The histological analysis was focussed on the MPS organs, liver and spleen. As shown by confocal microscopy images in Figs. 8 and 9 taken on liver and spleen slices respectively, iron uptake (Fig. 7) was co-localized with rhodamine-labelled liposome accumulation in the tissues. Organ structure was visualized by laser-beam excitation wavelength at 488 nm and emission recording in the 505–550 nm range, i.e., in the intrinsic fluorescence bands of the tissue and outside of those of Rho-PE (Fig. 1 and Martina et al., 2007). Rhodamine-labelled MFLs were revealed by laser-beam excitation wavelength at 543 nm and recording in the 563–659 nm range (see Figs. 1 and 2). In

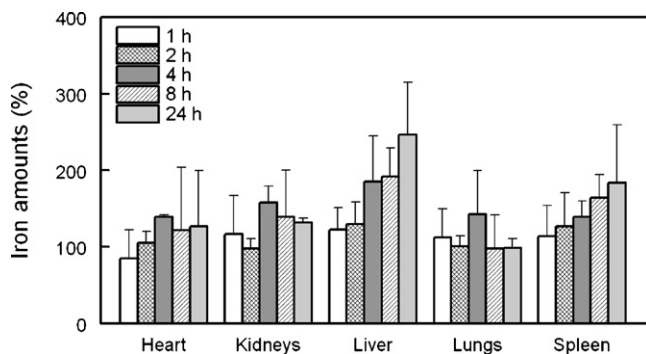


Fig. 7. Retention of iron in organs versus time after one intravenous injection of magnetic-fluid-loaded liposomes in mice (246 μ mol iron oxide and 145 μ mol lipids per kg). Iron amounts are expressed in percentage of the iron content found in organs of non-injected mice ($n=3$). Each bar is the mean value for three animals.

Fig. 8a, control images of liver from a non-injected mouse show perfect superimposition of intrinsic fluorescence of the tissue in the 505–550 nm range (excitation at 488 nm, seen in green) with rather weak and sparse auto-fluorescence in the 563–659 nm range (excitation at 543 nm, seen in red) due to protein prosthetic groups such as haem (Fig. 3). Consequently, areas with well localized fluorescence signals of high intensity (over the threshold of auto-fluorescence of the tissues) detected after excitation at 543 nm can be interpreted as corresponding to concentrated Rho-PE which is still within an intact MFL membrane (Martina et al., 2007; Riviere et al., in press).

Fig. 8b and c show typical images of liver slices at 4 h after injection. Fluorescent spots can be seen inside the blood vessels in both longitudinal (Fig. 8b) and transversal (Fig. 8c) sections. These spots correspond to Rho-PE MFLs because of their high fluorescence intensity and since most of them coincide to black areas at 488-nm excitation. In Fig. 8c, sparser but intense fluorescence detected in the parenchyma only at 543-nm excitation indicates extravasation of part of the MFLs. After 24 h, MFLs were only seen inside the vessels (Fig. 8d). A micrograph typical of a spleen slice from a control mouse is shown in Fig. 9a. Very little auto-fluorescence in the emission range of rhodamine was detected; therefore, as in liver, any bright spots visualized in treated mice would be due to the presence of fluorescent MFLs. An image recorded 4 h after injection clearly reveal MFLs located within red pulp and some starting to appear in white pulp (Fig. 9b) whereas at 24 h, the trapped liposomes were recovered only inside white pulp (Fig. 9c).

4. Discussion

The aim of this work was to study the pharmacokinetics and organ distribution of a new and promising formulation of magnetoliposomes. For this sort of investigation, it is essential to have reliable markers for the vesicles; ideally, both the lipid bilayer and the internal aqueous volume and content should be labelled (Allen et al., 1995). The phosphatidylethanolamine derivative Rho-PE is a good tracer of the lipid component since it inserts into phospholipid bilayers without inducing structural defects (Eidelman et al., 1988; Paternostre et al., 1995) and is stable in biological fluids, since it does not undergo exchange with plasma lipoproteins (Davidson et al., 2006; Torchilin, 2005). Furthermore, its chemical stability and high fluorescence sensitivity allowed us to develop a one-step determination of lipid concentrations from whole blood sample that has, to the best of our knowledge, not been described before. Moreover, the maghemite particles contained in the MFLs constituted an excellent tracer of liposome internal volume and content. Iron oxide can be easily detected by atomic absorption spectrometry in biological tissue extracts and in blood by relaxometry. The latter technique has been already applied (Weissleder et al., 1989) and its usefulness was confirmed here. It is worth noting that the only difficulty inherent to MFLs was their rather high density due to iron loading which made it impossible to recover them in the plasma by a centrifugation process. Therefore, it was important to develop techniques that could be used on whole blood. Another advantage of iron oxide particles as a marker was their

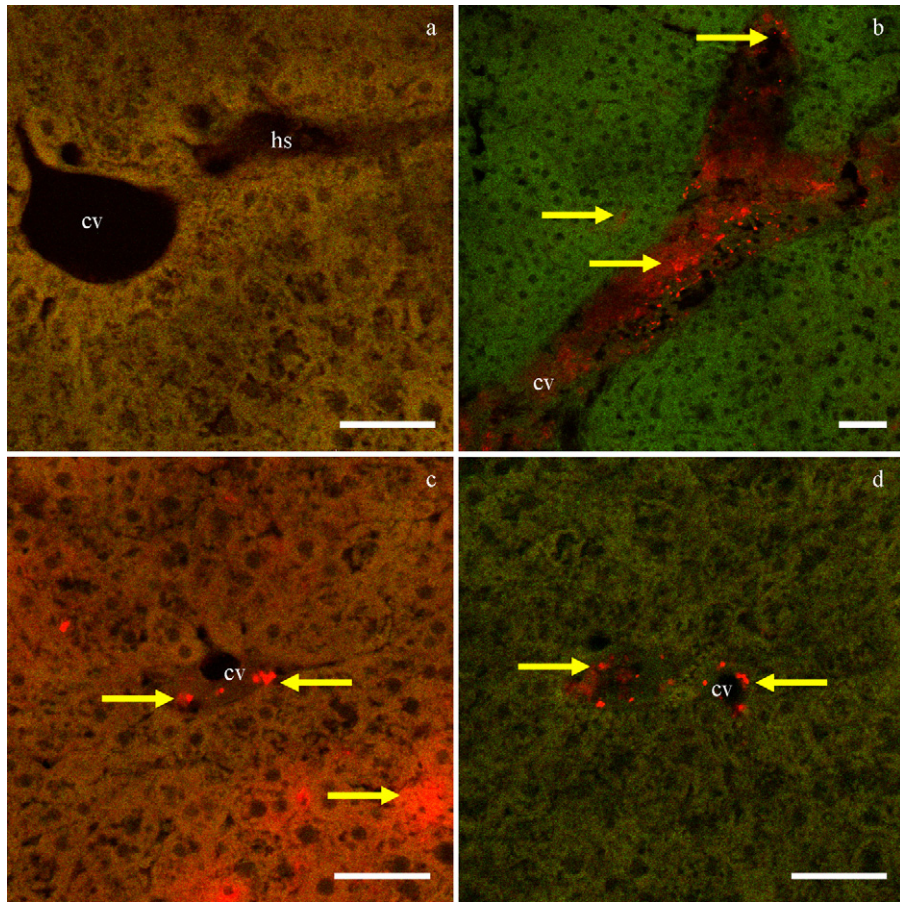


Fig. 8. Confocal microscopy images of liver slices from (a) a control mouse or (b–d) mice injected by magnetic-fluid-loaded liposomes at 4 h (b and c) and 24 h (d) before removing the organs (246 μmol iron oxide and 145 μmol lipids per kg). Red and green areas correspond to rhodamine fluorescence acquisition (excitation at 543 nm, collected emission in the 563–659 nm range) and tissue fluorescence acquisition (excitation at 488 nm, collected emission in the 505–550 nm range), respectively (magnification 40 \times (b) or 30 \times (a, c, and d)). White bars represent 50 μm . Letters show central veins (cv) or erythrocytes (hs) and yellow arrows localize Rho-PE MFLs.

retention within the liposome structure. With a diameter close to 8 nm, the maghemite particles are too large to cross the phospholipid bilayer passively and only leak when pores are formed in the bilayer (Lesieur et al., 2003). This gives them an advantage over low-molecular-mass tracers of the internal aqueous volume. The robustness of these two complementary techniques for following the MFLs allowed us to perform reliable pharmacokinetic and distribution experiments.

Quantitative and independent analyses of lipids and iron oxide led to a first conclusion that MFLs circulate intact within the intravascular compartment without degradation or permeabilization of the lipid membrane, since the initial magnetic fluid loading was maintained over a 24-h period of time. This is consistent with our previous, qualitative observations by magnetic resonance angiographic imaging (Martina et al., 2005). From a general point of view, this result gives reliable additional evidence more for *in vivo* structural resistance of PEG-ylated liposomes in blood. This can be explained by the now well accepted steric stabilizing effect of the hydrophilic polymeric chains which protect vesicles from their intrinsic susceptibility to aggregation and fusion and, to a certain extent, can delay the action of exogenous destabilizing components (Beugin-Deroo

et al., 1998; Needham et al., 1992). Here, the total retention of the loaded iron oxide particles within the internal vesicle volume after intravenous administration shows that the MFL bilayer was not damaged in blood stream.

The second conclusion of the pharmacokinetic study was to demonstrate the existence of two first-order kinetics of elimination with clearly different rate constants. This strongly resembled an elimination profile typically described by a two-compartment open model where there is a rapid distribution phase into the MPS followed by a slower elimination phase from the blood (Allen et al., 1995). In the case of MFLs, it is clear that the first phase of elimination corresponds to rapid uptake by liver and spleen, as shown by the tissue distribution of iron and organ histology. Interestingly, the liposome localisation with time in spleen, changed in a way similar to the migration of dendritic cells when they capture foreign material and present it to lymphocytes. This confirmed that MFLs were removed from the blood compartment via a phagocytic mechanism and thus did not exhibit strict “stealth” behaviour. In fact, hepatic and splenic sequestration within the first hour of injection has already been observed for other PEG-ylated vesicle systems (Moghimi and Szebeni, 2003; Gabizon et al., 1994;

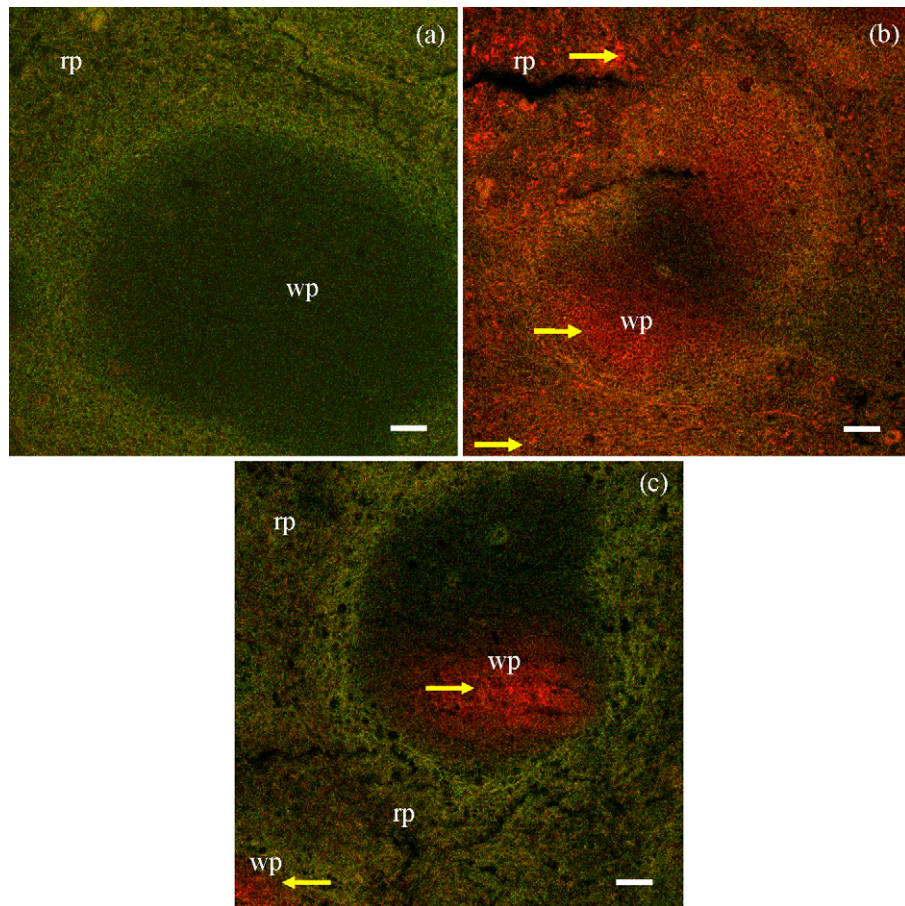


Fig. 9. Confocal microscopy images of spleen slices from (a) a control mouse or (b and c) mice injected by magnetic-fluid-loaded liposomes at 4 h (b) and 24 h (c) before removing the organ (246 μmol iron oxide and 145 μmol lipids per kg). Red and green areas correspond to rhodamine fluorescence acquisition (excitation at 543 nm, collected emission in the 563–659 nm range) and tissue fluorescence acquisition (excitation at 488 nm, collected emission in the 505–550 nm range), respectively (magnification 14 \times). White bars represent 50 μm . Letters show red pulp (rp) or white pulp (wp) and yellow arrows localize Rho-PE MFLs.

Gabizon, 1995). As recently suggested (Moghimi and Szebeni, 2003; Dos Santos et al., 2007), despite PEG grafting, adsorption of plasma proteins onto the liposome surface would be not totally impeded and opsonisation could occur efficiently *in vivo*. This first phase has worthwhile often been missed in pharmacokinetic studies since it requires the determination of liposome levels at very early time points after injection which has not usually been performed (Allen et al., 1995). It could be not totally ruled out that the 200 nm mean diameter of the vesicles could favour their uptake by the MPS. Reducing the size of MFLs may improve their stealth behaviour (Charois and Allen, 2003) but would decrease the magnetic fluid amount per liposome with the risk to make magnetic guidance unworkable. This could deserve further investigation.

The second elimination phase has been generally attributed to transitory saturation of the MPS (Moghimi and Szebeni, 2003) and, for MFLs, occurred from two hours after administration. At these times, steady MFL concentrations around 30% of the injected dose were still detected in the blood circulation. Thereafter, MFLs showed long-circulating behaviour with a half-life of 12.6 h. Interestingly, the dose of 4 μmol per mouse at which saturation step was observed was clearly higher than

that determined for conventional liposomes (not PEG-ylated) usually below 2 μmol while effective Stealth® liposomes show pharmacokinetics independent of the dose (Allen et al., 1995). PEG-ylated MFLs then seem intermediate stealth systems that would deserve examination of pharmacokinetics at different doses.

Nevertheless, whereas PEG grafting clearly governed the fate of intravenously administered MFLs (Fig. 6), maghemite loading seemed enhance their removal from the blood compartment, with however no apparent influence of the iron loading. This puzzling result could be explained by the osmotic effect of the concentrated iron oxide within the vesicles all the more so as maghemite nanocrystals were stabilized by citrate anions and then were negatively charged as shown by their zeta potential found close to -18 mV in buffer. The concentration gradient may indeed induce water to enter and the vesicles to swell, which may stretch the bilayer more than in empty vesicles. This may change the bilayer elasticity properties and then PEG chain conformation and dynamics, favorizing opsonin binding and thereby interactions with phagocytic cells (Morone et al., 2001).

In summary, this work contributed to the *in vivo* characterisation of fluorescent magnetic-fluid-loaded liposomes stabilized

by PEG coating. Their pharmacokinetics studied in intravenous injection into mice ranks MFLs, unilamellar and close to 200 nm in diameter, among “intermediate” stealth delivery systems. The fact that identical profiles were observed for the vesicle lipids and their internal content demonstrated conclusively that they circulated as intact structures. Despite their initial rapid uptake by macrophages within 50 min of injection, they exhibited a second longer phase of circulation time and remained detectable in blood up to 24 h after injection. Since these particles are designed to be guided to a site of interest by an external magnetic field, this moderately enhanced circulation time would be sufficient to give them a number of interesting biological applications. As our previous results show, such particles can be directed *in vivo* by a magnet through the blood vessels towards solid tumors or into brain (Fortin et al., 2006; Riviere et al., *in press*; Martina et al., 2007). When loaded with a suitable therapeutic agent, such MFLs could be used to treat tumors and other pathologies efficiently, allowing overall drug doses to be reduced and avoiding side effects.

Acknowledgments

We thank D. Talbot (UMR CNRS 7612, Université Paris 6, France) for iron dosage and V. Nicolas (plateau technique-Imagerie cellulaire IFR141, Université Paris-Sud, France) for technical assistance in confocal microscopy as well as F. Gazeau (UMR CNRS 7057, Université Paris 7, France) and O. Clément (Unité INSERM U494, Faculté de Médecine Enfants Malades, Paris, France) for lending the Brucker spectrometer used for relaxometry. Organ sections cutting by cryomicrotome was performed in INSERM U689 laboratory (Hôpital Lariboisière, Paris, France). This work was supported by a grant of the Ministry of Research in France.

References

Allen, T.M., Cullis, P.R., 2004. Drug delivery systems: entering the mainstream. *Science* 303, 1818–1822.

Allen, T., Hansen, C.B., Lopes de Menezes, D.E., 1995. Pharmacokinetics of long-circulating liposomes. *Adv. Drug Deliv. Rev.* 16, 27–284.

Beugn-Deroo, S., Ollivon, M., Lesieur, S., 1998. Bilayer stability and impermeability of nonionic surfactant vesicles sterically stabilized by PEG–cholesterol conjugates. *J. Colloid Interface Sci.* 202, 324–333.

Canonne-Hergaux, F., Gros, P., 2002. Expression of the iron transporter DMT1 in kidney from normal and anemic mice. *Kidney Int.* 62, 147–156.

Charois, G.J.R., Allen, T.M., 2003. Rate of biodistribution of Stealth® liposomes to tumor and skin: influence of liposome diameter and implications for toxicity and therapeutic activity. *Biochim. Biophys. Acta* 1609, 102–108.

Davidson, S.W., Ghering, A.B., Beish, L., Tubb, M.R., Hui, D.Y., Pearson, K., 2006. The biotin-capture lipid affinity assay: a rapid method for determining lipid binding parameters for apolipoproteins. *J. Lipid Res.* 47, 440–449.

Dos Santos, N., Allen, C., Doppen, A.M., Anantha, M., Cox, K.A., Gallagher, R.C., Karlsson, G., Edwards, K., Kenner, G., Lacey, S., Webb, M.S., Bally, M.B., 2007. Influence of poly(ethylene glycol) grafting density and polymer length on liposomes: relating plasma circulating lifetimes to protein binding. *Biochim. Biophys. Acta* 1768, 1367–1377.

Eidelman, O., Blumenthal, R., Walter, A., 1988. Composition of octyl glucoside-phosphatidylcholine mixed micelles. *Biochemistry* 27, 2839–2846.

Fortin, J.P., Martina, M.S., Gazeau, F., Menager, C., Wilhelm, C., Bacri, J.C., Lesieur, S., Clément, O., 2006. Magnetic targeting of magnetoliposomes in solid tumors with MRI monitoring in mice—feasibility. *Radiology* 239, 415–424.

Gabizon, A., Catane, R., Uziely, B., Kaufman, B., Safra, T., Cohen, R., Martin, F., Huang, A., Barenholz, Y., 1994. Prolonged circulation time and enhanced accumulation in malignant exudates of doxorubicin encapsulated in polyethylene-glycol coated liposomes. *Cancer Res.* 54, 987–992.

Gabizon, A., 1995. Liposome circulation time and tumor targeting: implications for cancer chemotherapy. *Adv. Drug Deliv. Rev.* 16, 285–294.

Kuznetsov, A.A., Filippov, V.I., Alyautdin, R.N., Torshina, N.L., Kuznetsov, O.A., 2001. Application of magnetic liposomes for magnetically guided transport of muscle relaxants and anti-cancer photodynamic drugs. *J. Magn. Magn. Mater.* 225, 95–100.

Lakowicz, J.R., 1983. *Principles of Fluorescence Spectroscopy*. Plenum Press, New York, pp. 19–49, (Chapter 2).

Lasic, D.D., 1998. Novel applications of liposomes. *Trends Biotechnol.* 16, 307–321.

Leserman, L.D., Barbet, J., Kourilsky, F., Weinstein, J.N., 1980. Targeting to cells of fluorescent liposomes covalently coupled with monoclonal antibody or protein A. *Nature* 288, 602–604.

Martina, M.S., Fortin, J.P., Ménager, C., Cabuil, V., Dadhi, D., Pierrot, P., Edwards, K., 2003. Evidence of surfactant-induced formation of transient pores in lipid bilayers by using magnetic-fluid-loaded liposomes. *J. Am. Chem. Soc.* 125, 5266–5267.

Martina, M.S., Fortin, J.P., Ménager, C., Clément, O., Barratt, G., Grabielle-Madelmont, C., Gazeau, F., Cabuil, V., Lesieur, S., 2005. Generation of superparamagnetic liposomes revealed as highly efficient MRI contrast agent for *in vivo* imaging. *J. Am. Chem. Soc.* 127, 10676–10685.

Martina, M.S., Fortin, J.P., Fournier, L., Menager, C., Gazeau, F., Clement, O., Lesieur, S., 2007. Magnetic targeting of rhodamine-labeled superparamagnetic liposomes to solid tumors: *in vivo* tracking by fibered confocal fluorescence microscopy. *Mol. Imaging* 6, 140–146.

Massart, R., US patent 4329241, (1982).

Moghimi, S.M., Szebeni, J., 2003. Stealth liposomes and long circulating nanoparticles: critical issues in pharmacokinetics, opsonization and protein-binding properties. *Prog. Lipid Res.* 42, 463–478.

Morandat, S., El Kirat, K., 2007. Solubilization of supported lipid membranes by octyl glucoside observed by time-lapse atomic force microscopy. *Colloids surf. B* 55, 179–184.

Morone, N., Okumura, Y., Sunamoto, J., 2001. Mobility of poly(ethylene oxide) segments on surface of lecithin liposomes. *J. Bioact. Compat. Polym.* 16, 194–205.

Needham, D., Hristova, K., McIntosh, T.J., Dewhirst, M., Wu, N., Lasic, D.D., 1992. Polymer-grafted liposomes: physical basis for the “stealth” property. *J. Liposome Res.* 2, 411–430.

Nobuto, H., Sugita, T., Shimose, S., Yasunaga, Y., Murakami, T., Ochi, M., 2004. Evaluation of systemic chemotherapy with magnetic liposomal doxorubicin and a dipole external electromagnet. *Int. J. Cancer* 109, 627–635.

Okuata, Y., 1999. Delivery of diagnostic agents for magnetic resonance imaging. *Drug Deliv. Rev.* 37, 121–137.

Papahadjopoulos, D., Allen, T.M., Gabizon, A., Mayhew, E., Matthay, K., Huang, S.K., Lee, K.D., Woodle, M.C., Lasic, D.D., Redemann, C., Martin, F.J., 1991. Sterically stabilized liposomes: Improvements in pharmacokinetics and antitumor therapeutic efficacy. *Proc. Natl. Acad. Sci. U.S.A.* 88, 11460–11464.

Paternostre, M., Meyer, O., Grabielle-Madelmont, C., Lesieur, S., Ghanam, M., Ollivon, M., 1995. Partition coefficient of a surfactant between aggregates and solution: application to the micelle-vesicle transition of egg phosphatidylcholine and octyl beta-D-glucopyranoside. *Biophys. J.* 69, 2476–2488.

Riviere, C., Martina, M.S., Tomita, Y., Wilhem, C., Tran Dinh, A., Menager, C., Pinard, E., Lesieur, S., Gazeau, F., Seylaz, J., *in press*. Magnetic targeting

of nanometric magnetic-fluid-loaded liposomes to the mouse brain cortex. *Radiology*.

Shinkai, M., Ito, A., 2004. Functional magnetic particles for medical application. *Adv. Biochem. Eng. Biotechnol.* 91, 191–220.

Sluiter, W., Oomens, L.W., Brand, A., Van Furth, R., 1984. Determination of blood volume in the mouse with ^{51}Cr -labelled erythrocytes. *J. Immunol. Methods* 73, 221–225.

Torchilin, V.P., 2005. Fluorescence microscopy to follow the targeting of liposomes and micelles to cells and their intracellular fate. *Adv. Drug Deliv. Rev.* 57, 95–109.

Weissleder, R., Stark, D.D., Engelstad, B.L., Bacon, B.R., Compton, C.C., White, D.L., Jacobs, P., Lewis, J., 1989. Superparamagnetic iron oxide: pharmacokinetics and toxicity. *Am. J. Roentgenol.* 152, 167–173.